Submitted to the
XXII International Symposium on Lepton-Photon Interactions at High Energy
June 30 – July 5, 2005, Uppsala, Sweden

Abstract: 275 **Session: QCD/HS**

Neutral strange particle production in deep inelastic scattering at HERA

ZEUS Collaboration

Abstract

Inclusive Λ, $\overline{\Lambda}$ and K^0_S production in deep inelastic ep scattering has been studied with the ZEUS detector at HERA using an integrated luminosity of $120\,\mathrm{pb}^{-1}$. Differential cross sections, baryon to antibaryon production asymmetry and baryon to meson production ratio have been measured in the laboratory system for $Q^2 > 25$ GeV^2. The measured transverse and longitudinal polarisation of Λ and $\bar{\Lambda}$ are consistent with zero.

1 Introduction

This paper investigates the production of the neutral strange particles Λ, $\overline{\Lambda}$ and K_S^0 in *ep* deep inelastic scattering (DIS) at ZEUS. Various differential cross sections have been measured and compared to a Monte Carlo (MC) simulation.

For HERA *ep* collisions, the presence of a proton in the initial state may lead to a hadronic final state enriched with baryons. By investigating the asymmetry of Λ and $\overline{\Lambda}$[1] production the likelihood of the initial baryon number being transferred to the Λ system in the detector region is studied. The baryon-to-meson ratio is also explored by measuring the Λ/K_S^0 production ratio, which can give additional information on the production of strange baryons.

The Λ polarisation has been investigated previously both experimentally [1] and theoretically [2–8] since the striking discovery of Λ polarisation in inclusive production processes in the 1970s [9, 10]. The weak decay of the Λ is self-analysing, in that the Λ polarisation can be measured in the $p\pi$ decay channel via the angular distribution of the decay products:

$$\frac{dN}{d\Omega} \propto \frac{1}{4\pi}(1 \pm \alpha P \cos\theta) \tag{1}$$

in the Λ rest frame, where $\alpha = 0.642 \pm 0.013$ [11] is the decay-asymmetry parameter and P is either the longitudinal or transverse polarisation. θ is the angle between the proton momentum, $\vec{p}$, and the Λ momentum, $\vec{P}_\Lambda$ (longitudinal polarisation), or between $\vec{p}$ and $\mathbf{n} = \vec{P}_{\text{beam}} \times \vec{P}_\Lambda$, where $\vec{P}_{\text{beam}}$ is the momentum of the electron beam (transverse polarisation). The measurement of polarisation can be used to test the fundamental properties of the nucleon and to study the mechanism of the quark to hadron fragmentation process.

2 Experimental setup

The data used for this measurement were collected by the ZEUS detector at the HERA *ep* collider during the running period 1996 – 2000, at $\sqrt{s} = 300$ GeV in 1996 – 97 and $\sqrt{s} = 318$ GeV in 1998 – 2000. The data corresponds to an integrated luminosity of $120\,\text{pb}^{-1}$.

A detailed description of the ZEUS detector can be found elsewhere [12]. A brief outline of the components that are most relevant for this analysis is given below.

Charged particles are tracked in the central tracking detector (CTD) [13], which operates in a magnetic field of $1.43\,\text{T}$ provided by a thin superconducting coil. The CTD

[1] Hereafter, both Λ and $\overline{\Lambda}$ are referred to as Λ, unless explicit comparison is made.

consists of 72 cylindrical drift chamber layers, organized in 9 superlayers covering the polar-angle[2] region $15^\circ < \theta < 164^\circ$. The transverse-momentum resolution for full-length tracks is $\sigma(p_T)/p_T = 0.0058 p_T \oplus 0.0065 \oplus 0.0014/p_T$, with p_T in GeV.

The high-resolution uranium–scintillator calorimeter (CAL) [14] consists of three parts: the forward (FCAL), the barrel (BCAL) and the rear (RCAL) calorimeters. Each part is subdivided transversely into towers and longitudinally into one electromagnetic section (EMC) and either one (in RCAL) or two (in BCAL and FCAL) hadronic sections (HAC). The smallest subdivision of the calorimeter is called a cell. The CAL energy resolutions, as measured under test-beam conditions, are $\sigma(E)/E = 0.18/\sqrt{E}$ for electrons and $\sigma(E)/E = 0.35/\sqrt{E}$ for hadrons (E in GeV).

3 DIS Event Selection

An observed DIS event is characterised by the scattered electron detected in the CAL. The scattered electron is identified with a neural network from the deposited energy in the CAL. The kinematic variables Q^2 and x were reconstructed using the double-angle method (DA) [15] which has the best resolution for medium- and high-Q^2 events. The variable y was reconstructed using both electron and Jacquet-Blondel (JB) [16] methods. The following requirements are applied offline to select DIS events:

- a scattered electron was found with energy above 10 GeV;
- an event was accepted only if the impact position (X, Y) of the scattered electron on the CAL satisfied $\sqrt{X^2 + Y^2} > 36$ cm;
- $38 < \delta < 65$ GeV, where $\delta = \sum_i (E_i - P_{Z,i})$ and the sum runs over the energy and longitudinal momentum of all CAL cells. This cut reduces the background from photoproduction and events with large radiative corrections;
- $Q^2_{\mathrm{DA}} > 25\,\mathrm{GeV}^2$;
- $\mid Z_{\mathrm{vertex}} \mid < 50$ cm to reduce background from non-ep collisions;
- $y_{\mathrm{JB}} > 0.02$ to improve the accuracy of DA reconstruction;
- $y_e < 0.95$ to remove events where a fake electron are in the FCAL;
- an electron track if $0.3 < \theta_e < 2.6$ or $\delta > 44$ GeV if θ_e is outside this region. This cut further suppresses events from non-ep interactions, photoproduction and fake DIS.

[2] The ZEUS coordinate system is a right-handed Cartesian system, with the Z axis pointing in the proton beam direction, referred to as the "forward direction", and the X axis pointing left towards the center of HERA. The coordinate origin is at the nominal interaction point.

4 Strange Particle Reconstruction

Neutral strange particles were reconstructed by requiring a vertex displaced from the primary vertex. The tracks fitted to this vertex were then investigated - the mass of the decaying particle was reconstructed from two oppositely charged tracks coming from the secondary vertex. Each secondary track was required to pass through at least five CTD superlayers. The transverse momentum corresponding to each charged track was required to be greater than 150 MeV and the absolute pseudorapidity in the laboratory frame was less than 1.5. These constraints ensured good track resolution and acceptance. Λ and K_S^0 may also be created in interactions with the wall of the beam pipe. To remove these events, a cut on the angle between the reconstructed candidate momentum and the vector joining the primary vertex to the secondary vertex was applied. This angle was restricted to be less than 0.2 rad.

Only Λ baryons that decayed to $p\pi$ (branching ratio $63.9 \pm 0.5\%$ [11]) were reconstructed. For the calculation of the invariant mass(M), the track with the larger momentum was assigned the mass of the proton while the other was assigned the mass of the charged pion. For the K_S^0 case, only decays to $\pi^+\pi^-$ (branching ratio $68.6 \pm 0.27\%$ [17]) were reconstructed. Both tracks were assigned the mass of the charged pion. Additional requirements are:

- $0.6 < P_T^{K_S^0,\Lambda} < 2.5$ GeV and $\mid \eta^{K_S^0,\Lambda} \mid < 1.2$, where $P_T^{K_S^0,\Lambda}$ and $\eta^{K_S^0,\Lambda}$ are the transverse momentum and the pseudorapidity of the reconstructed candidate in the laboratory frame;
- $\mathrm{M}(e^+e^-) > 50$ MeV to eliminate the Dalitz decays;
- $\mathrm{M}(p\pi) > 1.125$ GeV for the K_S^0 candidate selection. Here the mass of the proton is assigned to the track with larger momentum and the mass of pion to the other track. This cut is applied to eliminate Λ contamination of the K_S^0 signal;
- $\mathrm{M}(\pi^+\pi^-) > 0.475$ GeV for the Λ candidate selection. This cut is applied to remove K_S^0 contamination of the Λ signal.

5 Monte Carlo Simulation

Data were corrected for detector effects by using the ARIADNE 4.08 [18] MC interfaced to HERACLES 4.6.1 [19–22] via DJANGOH 1.1 [22]. The parton density functions were taken from the CTEQ4D set. The strangeness suppression factor, λ_s, is set to 0.3. ARIADNE is based on the Color Dipole Model in which QCD coherence effects are treated as the gluon bremsstrahlung in terms of radiation from colour dipoles between partons. The program uses the LUND string model [23] to simulate the fragmentation of the partons.

6 Definition of Cross Sections and Systematic Uncertainties

The Λ and K_S^0 cross sections were measured in the kinematic region $Q^2 > 25\,\mathrm{GeV}^2$, $0.02 < y < 0.95$, $0.6 < P_T^{K_S^0,\Lambda} < 2.5$ GeV and $\mid \eta^{K_S^0,\Lambda} \mid < 1.2$. The cross sections were defined as

$$\frac{d\sigma}{dY} = \frac{N}{A \cdot \mathcal{L} \cdot B \cdot \Delta Y}, \tag{2}$$

where N is the number of Λ and K_S^0 hadrons in a bin of size ΔY, A is the acceptance evaluated using the MC and $\mathcal{L}$ is the integrated luminosity. The branching ratios, B, were taken as $63.9 \pm 0.5\%$ and $68.6 \pm 0.27\%$ for $\Lambda \rightarrow p\pi$ and $K_S^0 \rightarrow \pi^+\pi^-$ decay channels, respectively.

The main sources which contribute to the systematic uncertainty were investigated. The total systematic error for each bin was calculated by combining in quadrature the individual contributions described below:

- the scattered electron energy was varied by $\pm$ 1 GeV. The changes of cross sections were generally 1 − 2%. The largest uncertainty (8%) was observed in the lowest x region;
- the value Q^2 calculated from the electron method compared with the DA method. This changes the cross sections generally by less than 1%. The effect in the low-x region was up to 5%;
- the lowest cut on δ was increased and decreased by 2 GeV. In most cases, the effect was about 1 − 2% ($\pm$ 4% contribution at the low-x region);
- contributions from variations of the requirements on Z_{vertex}, y_{JB}, P_T^{trk}, η^{trk}, the collinearity cut and the electron radius cut were considered. The effects arising from these cuts were typically below 1% except 2 − 3% changes in the low-p_T and high-Q^2 regions.

A 2% uncertainty due to the luminosity measurement was included for the cross section. The uncertainty related to the branching ratio was neglected.

7 Results and Discussions

The differential Λ and K_S^0 cross sections, $\Lambda/\overline{\Lambda}$ asymmetry and Λ/K_S^0 ratio as a function of p_T are shown in Fig. 1 (a-d). There is usually fair agreement of the cross sections when comparing the data with the ARIADNE prediction. For the K_S^0 cross section, ARIADNE overestimates the cross sections at lower p_T. Because of this, the Λ/K_S^0 ratio was also underestimated by the MC in the same p_T region. No significant $\Lambda/\overline{\Lambda}$ asymmetry was observed.

Figure 2 shows the same distributions as a function of η. Again, ARIADNE generally describes the Λ cross section but is above the cross section for K_S^0 production. The baryon to meson ratio has a tendency to increase with increasing η, whereas the MC is much more symmetric around $\eta = 0$. The data is consistent with no baryon-antibaryon asymmetry.

Similar distributions as a function of x are shown in Fig. 3. The $\Lambda/\overline{\Lambda}$ distribution indicates no baryon-antibaryon asymmetry. The baryon-to-meson ratio shows a steep rise in the Λ compared with K_S^0 production as x decreases - at the smallest x measured it is almost half as likely to get a baryon as a meson. ARIADNE underestimates this ratio in the lower x region, although the same trend is present. Fig. 4 shows the distributions as a function of Q^2. Again, there is no evidence for any baryon-antibaryon asymmetry. The Λ to K_S^0 ratio is not perfectly described by the MC.

The results on the Λ and $\overline{\Lambda}$ decay angular distributions are presented in Fig. 5 and 6. Averaged over the full kinematic range, the transverse polarisation of Λ and $\overline{\Lambda}$ were observed to be $+1.4 \pm 4.5(\text{stat.})^{+4.1}_{-1.9}(\text{syst.})\%$ and $-1.8 \pm 4.4(\text{stat.})^{+3.1}_{-1.3}(\text{syst.})\%$ respectively. The longitudinal polarisation of Λ and $\overline{\Lambda}$ was also measured to be consistent with zero within the total uncertainties. The longitudinal polarisation was observed to be $+0.3 \pm 10.3(\text{stat.})^{+0.1}_{-7.8}(\text{syst.})\%$ for Λ and $+19.8 \pm 10.8(\text{stat.})^{+4.2}_{-12.6}(\text{syst.})\%$ for $\overline{\Lambda}$.

8 Conclusions

Strange particle production in inclusive DIS has been studied in deep inelastic scattering in the kinematic range $Q^2 > 25\,\text{GeV}^2$, $0.02 < y < 0.95$, $0.6 < P_T^{K_S^0,\Lambda} < 2.5$ GeV and $|\ \eta^{K_S^0,\Lambda}\ | < 1.2$. ARIADNE gives a general description of the data for both Λ and K_S^0 production. There exists a phase space region however where this MC is not sufficient to describe the Λ/K_S^0 ratio, particularly at low p_T and low x. No significant baryon to antibaryon production asymmetry was observed. An obvious extension to this study is to further differentiate the sample, for example into the target and current regions of the Breit frame.

The measured transverse and longitudinal polarisation are both consistent with zero. The transverse polarisation reported here suggests that no preferential planes exist for Λ production, which in the model of DeGrand and Miettinen [2] leads to the conclusion that the strange quarks do not come from any particular direction.

References

[1] K. Heller, *In Proceedings of the 12th International Symposium on High Energy Spin Physics*, p. 23. Amsterdam, Netherlands, 1996. edited by C.W. DeJager, T.J. Ketel, P.J. Muders, J.E.J. Oberski and M. Oskam-Tamboezer (World Scientific, Singapore, 1997).

[2] T.A. DeGrand and H.I. Miettinen, Phys. Rev. **D 24**, 2419 (1981).

[3] J. Szwed, Phys. Lett. **B 105**, 403 (1981).

[4] L.G. Pondrom, Phys. Rep. **122**, 57 (1985).

[5] J. Soffer and N.A. Törnqvist, Phys. Rev. Lett. **68**, 907 (1992).

[6] Liang Zuo-tang and C. Boros, Phys. Rev. Lett. **79**, 3608 (1997).

[7] Liang Zuo-tang and C. Boros, Phys. Rev. **D 61**, 117503 (2000).

[8] M. Anselmino, D. Boer, U. D'Alesio and F. Murgia, Phys. Rev. **D 63**, 054029 (2001).

[9] A. Lesnik et al., Phys. Rev. Lett. **35**, 770 (1975).

[10] G. Bunce et al., Phys. Rev. Lett. **36**, 1113 (1976).

[11] S. Eidelman et al., Phys. Lett. **B 592**, 1 (2004).

[12] ZEUS Coll., U. Holm (ed.), *The ZEUS Detector*. Status Report (unpublished), DESY (1993), available on `http://www-zeus.desy.de/bluebook/bluebook.html`.

[13] N. Harnew et al., Nucl. Inst. Meth. **A 279**, 290 (1989);
B. Foster et al., Nucl. Phys. Proc. Suppl. **B 32**, 181 (1993);
B. Foster et al., Nucl. Inst. Meth. **A 338**, 254 (1994).

[14] M. Derrick et al., Nucl. Inst. Meth. **A 309**, 77 (1991);
A. Andresen et al., Nucl. Inst. Meth. **A 309**, 101 (1991);
A. Caldwell et al., Nucl. Inst. Meth. **A 321**, 356 (1992);
A. Bernstein et al., Nucl. Inst. Meth. **A 336**, 23 (1993).

[15] S. Bentvelsen, J. Engelen and P. Kooijman, *Proc. Workshop on Physics at HERA*, W. Buchmüller and G. Ingelman (eds.), Vol. 1, p. 23. Hamburg, Germany, DESY (1992);
K.C. Höger, *Proc. Workshop on Physics at HERA*, W. Buchmüller and G. Ingelman (eds.), Vol. 1, p. 43. Hamburg, Germany, DESY (1992).

[16] F. Jacquet and A. Blondel, *Proceedings of the Study for an ep Facility for Europe*, U. Amaldi (ed.), p. 391. Hamburg, Germany (1979). Also in preprint DESY 79/48.

[17] K. Hagiwara et al., Phys. Rev. **D 66**, 010001 (2002).

[18] L. Lönnblad, Comp. Phys. Comm. **71**, 15 (1992).

[19] A. Kwiatkowski, H. Spiesberger and H.-J. Möhring, Comp. Phys. Comm. **69**, 155 (1992). Also in *Proc. Workshop Physics at HERA*, 1991, DESY, Hamburg.

[20] K. Charchula, G.A. Schuler and H. Spiesberger, Comp. Phys. Comm. **81**, 381 (1994).

[21] H. Spiesberger, *An Event Generator for ep Interactions at HERA Including Radiative Processes (Version 4.6)*, 1996, available on `http://www.desy.de/~hspiesb/heracles.html`.

[22] H. Spiesberger, HERACLES *and* DJANGOH*: Event Generation for ep Interactions at HERA Including Radiative Processes*, 1998, available on `http://www.desy.de/~hspiesb/djangoh.html`.

[23] B. Andersson et al., Phys. Rep. **97**, 31 (1983).

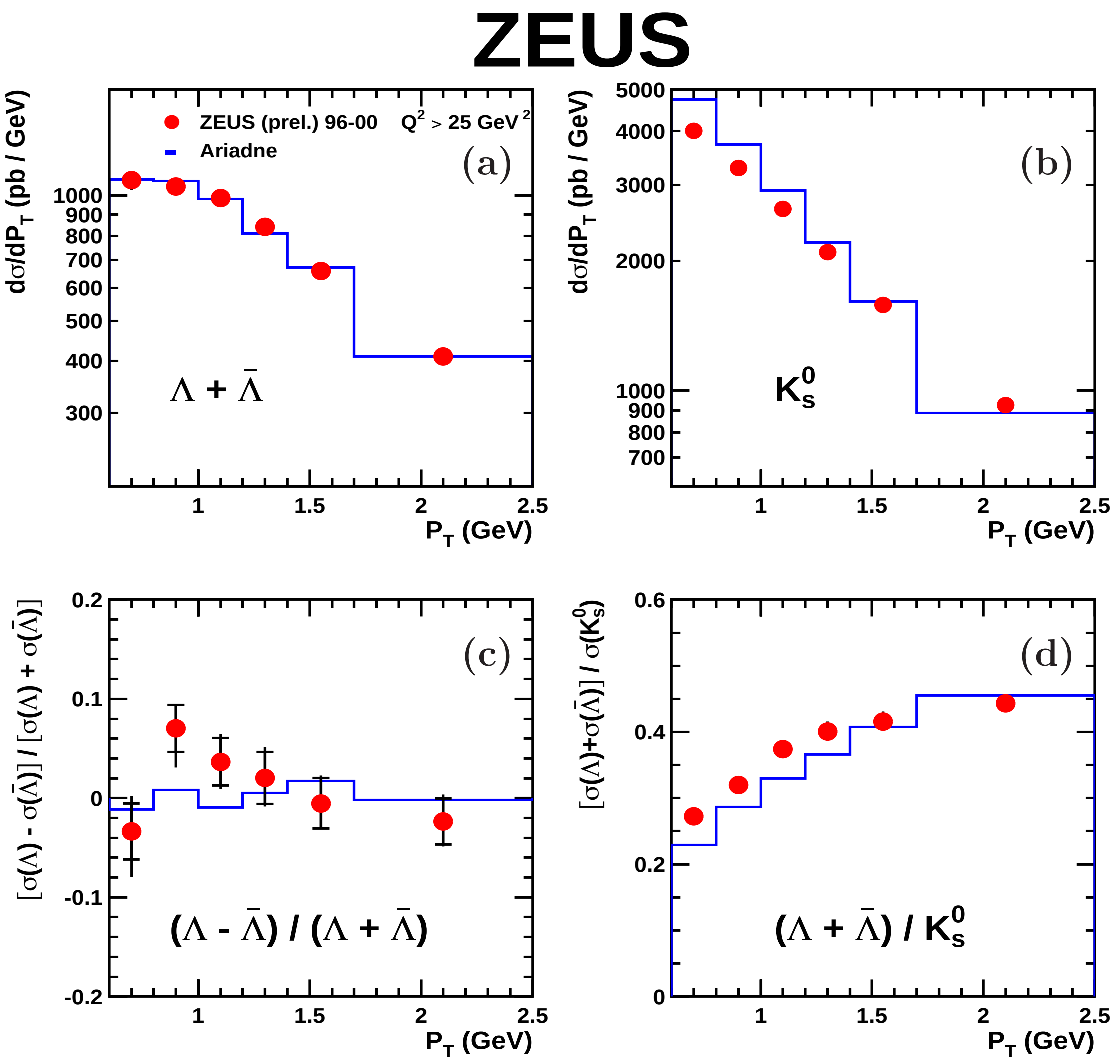

Figure 1: *Cross sections and ratios as a function of p_T in the kinematic region given by $Q^2 > 25\,GeV^2$ and $0.02 < y < 0.95$: a) The measured differential cross sections $d\sigma/dP_T$ for $ep \to e + \Lambda + X$ compared with ARIADNE. b) The measured differential cross sections $d\sigma/dP_T$ for $ep \to e + K^0_S + X$ compared with ARIADNE. c)The production asymmetry of Λ to $\bar{\Lambda}$. d) The ratio of $(\Lambda + \overline{\Lambda})/K^0_S$. The inner error bars show the statistical uncertainties and the full bars the statistical and systematic uncertainties added in quadrature.*

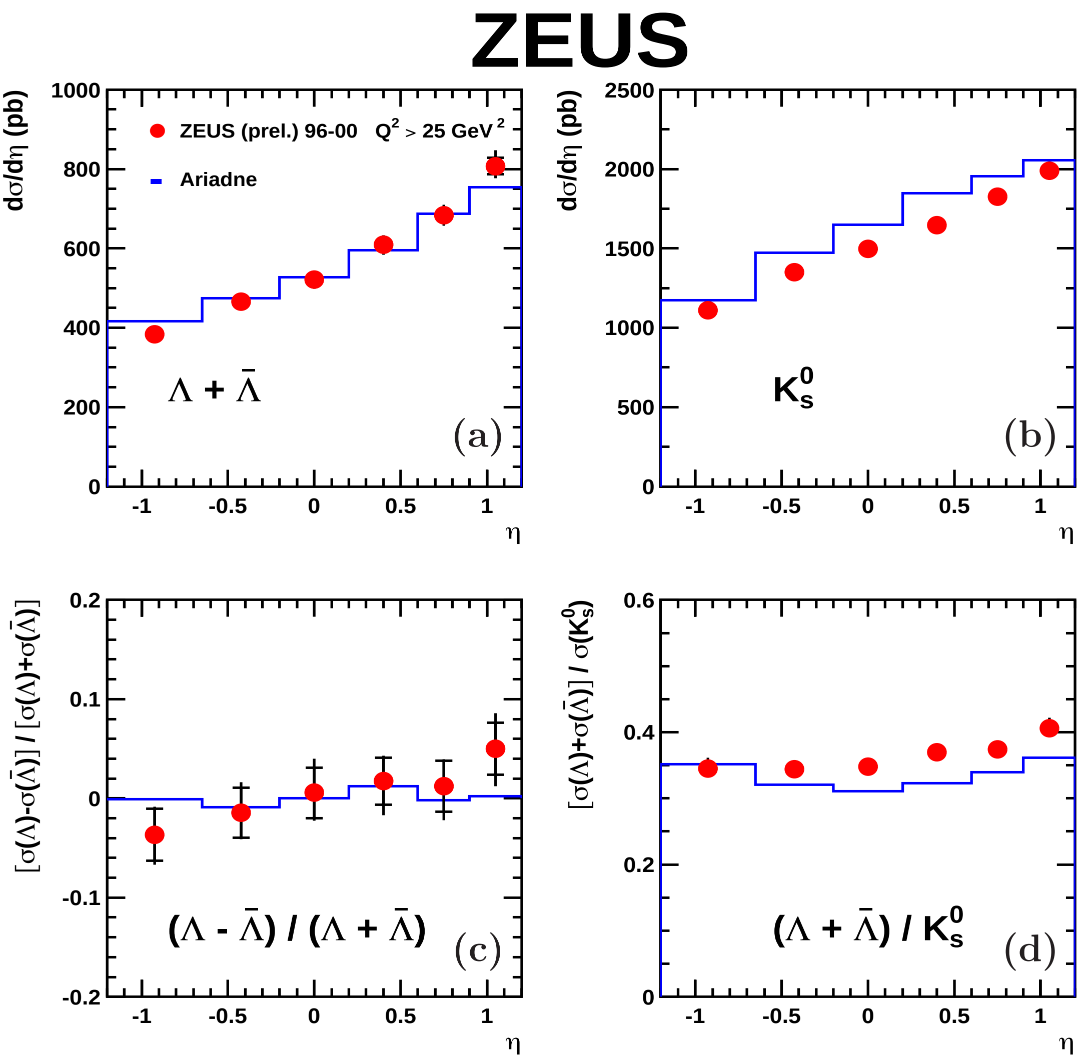

Figure 2: *Cross sections and ratios as a function of η in the kinematic region given by $Q^2 > 25\,GeV^2$ and $0.02 < y < 0.95$: a) The measured differential cross sections $d\sigma/d\eta$ for $ep \to e + \Lambda + X$ compared with ARIADNE. b) The measured differential cross sections $d\sigma/d\eta$ for $ep \to e + K^0_S + X$ compared with ARIADNE. c)The production asymmetry of Λ to $\bar{\Lambda}$. d) The ratio of $(\Lambda + \overline{\Lambda})/K^0_S$. The inner error bars show the statistical uncertainties and the full bars the statistical and systematic uncertainties added in quadrature.*

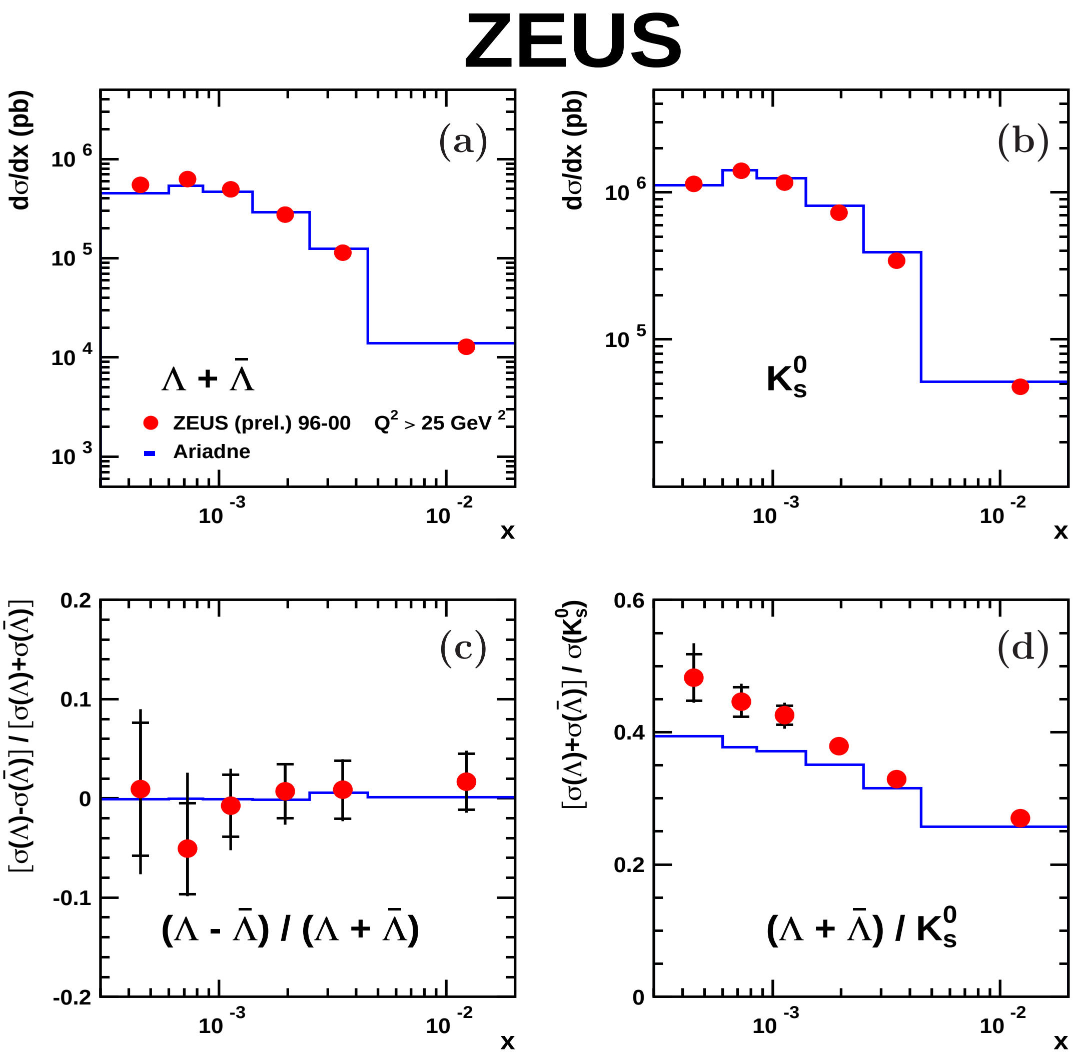

Figure 3: *Cross sections and ratios as a function of x in the kinematic region given by $Q^2 > 25\,GeV^2$ and $0.02 < y < 0.95$: a) The measured differential cross sections $d\sigma/dx$ for $ep \to e + \Lambda + X$ compared with ARIADNE. b) The measured differential cross sections $d\sigma/dx$ for $ep \to e + K^0_S + X$ compared with ARIADNE. c)The production asymmetry of Λ to $\bar{\Lambda}$. d) The ratio of $(\Lambda + \bar{\Lambda})/K^0_S$. The inner error bars show the statistical uncertainties and the full bars the statistical and systematic uncertainties added in quadrature.*

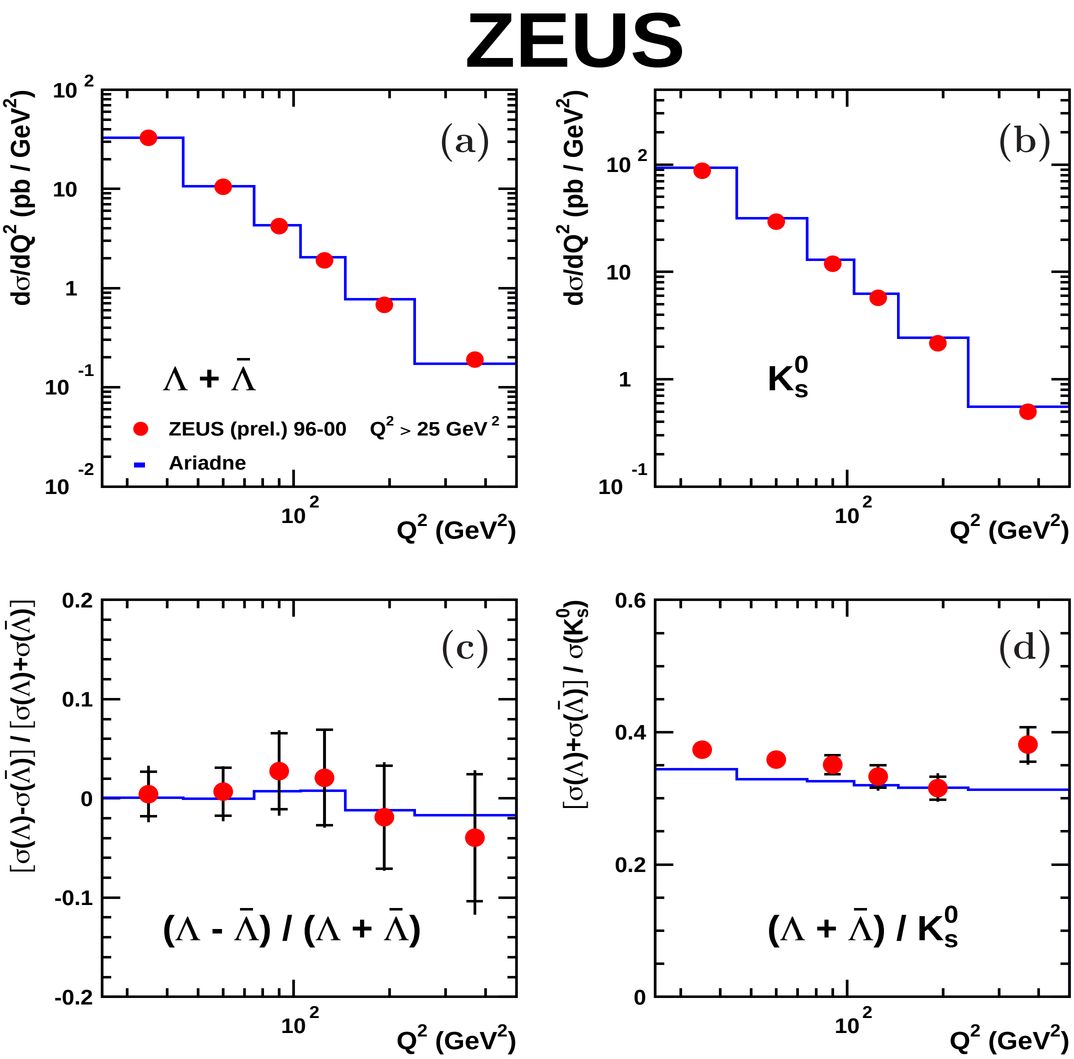

Figure 4: *Cross sections and ratios as a function of Q^2 in the kinematic region given by $Q^2 > 25\,GeV^2$ and $0.02 < y < 0.95$: a) The measured differential cross sections $d\sigma/dQ^2$ for $ep \rightarrow e + \Lambda + X$ compared with ARIADNE. b) The measured differential cross sections $d\sigma/dQ^2$ for $ep \rightarrow e + K^0_S + X$ compared with ARIADNE. c)The production asymmetry of Λ to $\bar{\Lambda}$. d) The ratio of $(\Lambda + \overline{\Lambda})/K^0_S$. The inner error bars show the statistical uncertainties and the full bars the statistical and systematic uncertainties added in quadrature.*

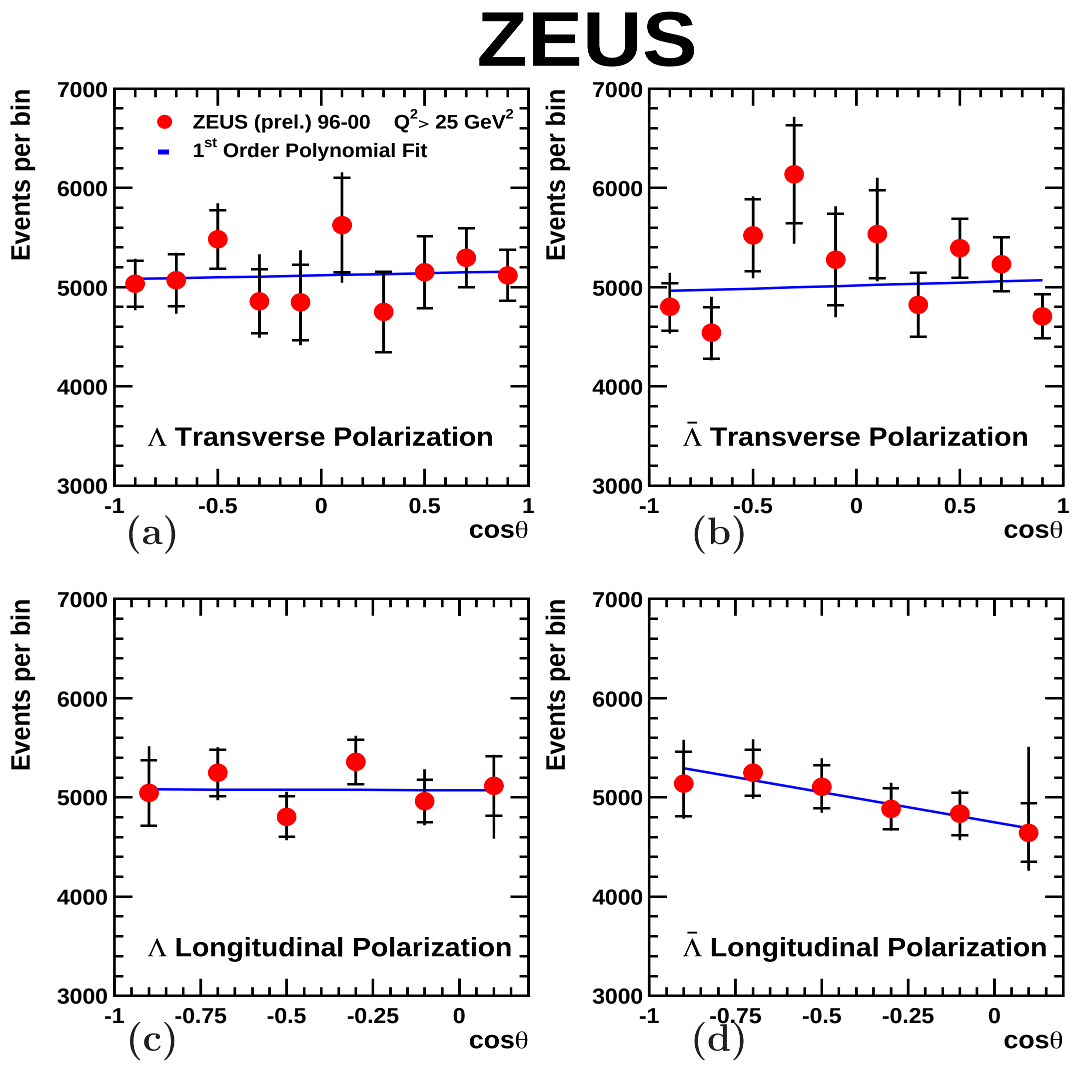

Figure 5: *Λ and $\bar{\Lambda}$ polarisations in the kinematic region given by $Q^2 > 25\,GeV^2$ and $0.02 < y < 0.95$.*

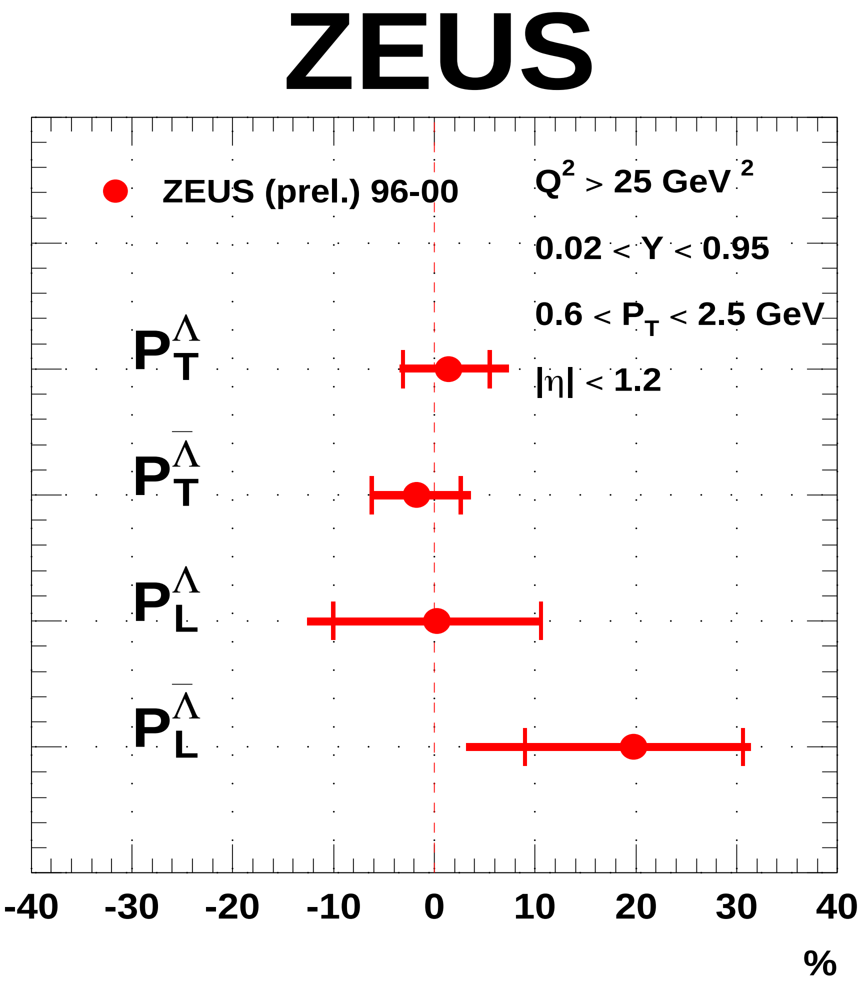

Figure 6: *Λ and $\bar{\Lambda}$ polarisations. The inner error bars show the statistical uncertainties and the full bars the statistical and systematic uncertainties added in quadrature.*